

370 New Insights and Animal models

Tuesday, May 09, 2017 3:45 PM–5:30 PM

Room 314 Paper Session

Program #/Board # Range: 3422–3428**Organizing Section:** Genetics Group**Program Number:** 3422**Presentation Time:** 3:45 PM–4:00 PM**Alternative splicing of mRNA regulated by Musashi is crucial for photoreceptor development and function**Jesse Sundar^{1,2}, Peter Stoilov¹, Visvanathan Ramamurthy^{1,2}.¹Biochemistry and Molecular Biology, West Virginia University, Morgantown, WV; ²Ophthalmology, West Virginia University, Morgantown, WV.

Purpose: The mechanisms that drive the production of photoreceptor-specific protein isoforms and their roles in photoreceptor function are poorly understood. Our previous studies suggest that photoreceptor-specific protein isoforms are needed for development of the outer segment (OS). In addition, our data implicated a role for Musashi, a family of RNA-binding proteins, in promoting the inclusion of photoreceptor-specific exons. Therefore, we hypothesized that the Musashi proteins are required for the morphogenesis and function of photoreceptor cells.

Methods: We generated retina-specific knockout mice in which either Musashi-1 (Msi1), Musashi-2 (Msi2), or both genes were ablated. After validating these models by western blot, we analyzed their photoreceptor function by electroretinography (ERG) and their morphology by immunocytochemistry. The splicing of photoreceptor-specific exons in mature transcripts was determined by reverse transcriptase PCR. Statistical analyses were performed using the two-tailed student's t-test.

Results: Photoreceptor function was absent in the Msi1/Msi2 double knockout mice at postnatal day 16, which was the earliest time point that we tested (n=3) (Fig. 1). The loss of function correlated with disrupted photoreceptor OS development in double knockout mice (n=3). Lastly, the inclusion of 13 out of 14 photoreceptor specific exons that we tested was blocked in the double knockout mice. In contrast to the double knockout, photoreceptor function and morphology was mostly preserved at postnatal day 16 in the single Msi1 or Msi2 knockouts. The Msi1 but not Msi2 single knockout had a moderate effect on exon inclusion for some of the alternative exons tested.

Conclusions: Our results show that the Musashi proteins are required for normal photoreceptor development and likely control the photoreceptor-specific splicing program. We also observed significant functional redundancy of the two Musashi genes in photoreceptor cells.

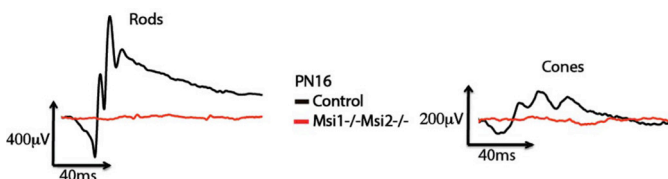


Figure 1: Scotopic and photopic ERGs showing absence of the light-dependent photoreceptor response in the Msi1/Msi2 double knockout mouse compared to littermate control.

Commercial Relationships: Jesse Sundar, None; Peter Stoilov, None; Visvanathan Ramamurthy, None

Support: R01EY025536 and R01EY017035

Program Number: 3423**Presentation Time:** 4:00 PM–4:15 PM**Complex interaction and Hardy-Weinberg disequilibrium of ABCA4 disease-causing alleles provides insights into the pathogenesis of retinopathy**Ana Fakin^{1,2}, Valentina Cipriani^{1,2}, Stanley Lambertus³, Nathalie Bax³, Anthony G. Robson^{1,2}, Kaoru Fujinami^{1,4}, John Chiang⁵, Anthony T. Moore^{1,6}, Michel Michaelides^{1,2}, Graham E. Holder^{1,2}, Carel C. Hoyng³, Andrew R. Webster^{1,2}.

¹UCL Institute of Ophthalmology, London, United Kingdom; ²Moorfields Eye Hospital, London, United Kingdom; ³Department of Ophthalmology, Donders Institute for Brain, Cognition and Behaviour, Radboud university medical center, Nijmegen, Netherlands; ⁴National Institute of Sensory Organs, National Hospital Organization, Tokyo Medical Center, Tokyo, Japan; ⁵Casey Molecular Diagnostic laboratory, Portland, OR; ⁶Department of Ophthalmology, UCSF School of Medicine, San Francisco, CA.

Purpose: A paradox exists between the prevalence of disease-associated *ABCA4* alleles in affected patients on the one hand, and their relative ratios in the population on the other. We explore this phenomenon in two large patient populations and the ExAC database. We determine genotype-phenotype correlations.

Methods: Study included 397 probands from Moorfields Eye Hospital (MEH) and 166 probands from Radboud university medical center (Radboudumc) with a clinical presentation of *ABCA4*-retinopathy and two pathogenic *ABCA4* alleles. The ratio of genotypes comprising null and missense alleles was determined and compared with the ratio expected according to the population data (Exac.broadinstitute.org). The analysis was repeated for 15 alleles (14 missense, 1 splicing) of known severity (Fakin et al, IOVS 2016). Phenotypes of 210 patients with two of the above and/or null alleles were studied with electrophysiology (ERG; departure from the null phenotype) and fundus autofluorescence (frequency of foveal sparing, FS).

Results: Assuming Hardy-Weinberg equilibrium, the expected ratio of null/null, null/missense and missense/missense genotypes was 1:35:298, and the observed 1:6:7. The expected ratio of severe/severe, severe/mild and mild/mild genotypes was 1:20:128, and the observed 1:1.5:0.1. Specifically, there was a disequilibrium for two allele classes: (1)p.G863A, p.L2027F, c.5714+5G>A, and (2)p.G1961E: these occurred in homozygous, (1)/(1) or (2)/(2), but never in compound heterozygous state (1)/(2). Analysis of phenotypes suggested that the first retained higher *ABCA4* function in foveal cones (high frequency of FS), whereas p.G1961E retained higher *ABCA4* function in the extrafoveal retina (high frequency of normal ERG). Findings were replicated in the Radboudumc cohort.

Conclusions: The skewed genotype ratios suggest incomplete penetrance for a large number of pathogenic *ABCA4* alleles, depending on the nature of the second allele. Many people harboring two pathogenic *ABCA4* alleles may thus be unaffected or have an unrecognized phenotype that does not lead to a referral to a specialist clinic. Further, allele classes that cause different phenotypes in homozygous state and do not occur in *trans* suggest that *ABCA4* protein has at least two functions, which can be affected unequally and in some instances reciprocally compensated.

Commercial Relationships: Ana Fakin, None; Valentina Cipriani, None; Stanley Lambertus, None; Nathalie Bax, None; Anthony G. Robson, None; Kaoru Fujinami, None; John Chiang, None; Anthony T. Moore, None; Michel Michaelides, None; Graham E. Holder, None; Carel C. Hoyng, None; Andrew R. Webster, None

Support: National Institute for Health Research Rare Diseases Translational Research Collaboration (NIHR RD-TRC), Cambridge

Program Number: 3424

Presentation Time: 4:15 PM–4:30 PM

Genetic Variation in RRAGC Affects Progression Rate from Intermediate to Advanced Age-Related Macular Degeneration

William K. Scott¹, Patrice Persad¹, Rebecca J. Sardell¹, Samuel S. Pan¹, Patrice W. Gay¹, Larry D. Adams¹, Renee Laux², Jorge Fortun³, Milam A. Brantley⁴, Jaclyn L. Kovach³, Stephen G. Schwartz³, Anita Agarwal^{4,5}, Jonathan L. Haines², Margaret A. Pericak-Vance¹. ¹John P. Hussman Institute for Human Genomics, University of Miami, Miami, FL; ²Department of Epidemiology and Biostatistics, Case Western Reserve University, Cleveland, OH; ³Bascom Palmer Eye Institute, University of Miami, Miami, FL; ⁴Ophthalmology and Visual Sciences, Vanderbilt University Medical Center, Nashville, TN; ⁵West Coast Retina, San Francisco, CA.

Purpose: Genome-wide association studies examining progression rate from intermediate to advanced age-related macular degeneration (AMD) are lacking. Most published studies on AMD progression rate feature known AMD risk loci, which may not fully explain progression rate variability among patients, and combine early and intermediate AMD cases together, introducing phenotypic heterogeneity. This study aims to identify novel progression loci with a focus on phenotypic subtypes that have drusen as prominent characteristics at baseline.

Methods: We studied 397 European-descended subjects (606 eyes with intermediate AMD at baseline, 178 of which progressed) with ≥ 2 examinations and a mean follow-up time of 2.5 years (range 0.05-13). Mean age at baseline was 76.5 years, and 58% of subjects were female. Genome-wide genotyping utilized the Illumina HumanCoreExome array and the dataset was imputed to 6.3 million single nucleotide polymorphisms (SNPs), with imputation quality (R^2) >0.3 and minor allele frequency ≥ 0.05 , using IMPUTE2 and the 1000 Genomes Project Phase I reference panel. Cox proportional hazards regression models were used to assess association of imputed SNP dosage with time to progression in each eye from intermediate AMD (extensive intermediate-size drusen or any large drusen) to advanced AMD (geographic atrophy or choroidal neovascularization). Non-progressors were censored at time of last examination. Models included the top two principal components from population stratification analyses, sex, and age at baseline, and accounted for correlation between an individual's eyes.

Results: Thirteen SNPs (in strong linkage disequilibrium) in the *RRAGC* gene on chromosome 1 had genome-wide significant main effects (at rs188028731, $p=1.2 \times 10^{-9}$, hazard ratio=3.1, 95% CI=2.2-4.5). These SNPs were associated with a shorter time to progression. Two other intergenic regions on chromosomes 3 ($p=3.2 \times 10^{-8}$) and 12 ($p=8.5 \times 10^{-10}$) produced genome-wide significant results. The 52 known AMD risk variants were not statistically significant.

Conclusions: *RRAGC* regulates mTORC1 signaling. This pathway influences neovascularization in AMD and is a target for drug development. Thus, identification of *RRAGC* as a progression locus may facilitate development of strategies for slowing progression rate from intermediate AMD to advanced AMD, slowing vision loss, and improving management of the disease in patients.

Commercial Relationships: William K. Scott, None; Patrice Persad, None; Rebecca J. Sardell, None; Samuel S. Pan, None; Patrice W. Gay, None; Larry D. Adams, None; Renee Laux, None; Jorge Fortun, None; Milam A. Brantley, None; Jaclyn L. Kovach, None; Stephen G. Schwartz, Alimera Sciences (C); Anita Agarwal, None; Jonathan L. Haines, None; Margaret A. Pericak-Vance, None
Support: NIH Grant EY012118

Program Number: 3425

Presentation Time: 4:30 PM–4:45 PM

Nature of the endophenotypes associated with the modifier for age-at-onset of glaucoma mapping at 20q13

Vincent Raymond^{1,2}, Pascal Belleau¹, Rose Arseneault¹, Stéphane Dubois³, Jean-Louis Anctil⁴, Gilles Côté⁴, Marcel Amyot⁵, Fahed Elian⁶, Michael A. Walter⁶. ¹Neurosciences, CHUL at CHU de Québec - Université Laval, Québec City, QC, Canada; ²Molecular Medicine, Université Laval, Québec City, QC, Canada; ³Endocrinology and Nephrology, CHUL at CHU de Québec - Université Laval, Québec City, QC, Canada; ⁴Ophthalmology, Université Laval, Québec City, QC, Canada; ⁵Ophthalmology, Université de Montréal, Montréal, QC, Canada; ⁶Medical Genetics, University of Alberta, Edmonton, AB, Canada.

Purpose: We studied a large autosomal dominant open-angle glaucoma (OAG) pedigree in which heterozygotes (HTZ) for the myocilin *MYOC*^{K423E} mutation displayed wide phenotypic variability. Diagnoses ranged from juvenile- (JOAG) to late-adult onset primary OAG (POAG) and several asymptomatic elderly HTZ were ≥ 55 years old. Our goals were to map modifier(s) interacting with *MYOC* and to define the altered endophenotypes.

Methods: 375 members of the French-Canadian CA family were screened for mutations. Ocular records of all carriers were obtained. 4 quantitative traits were defined as endophenotypes: age of maximal intra-ocular pressures (IOP_{max}), IOP progression, progression of cup to disk ratios and, age-at-onset (AAO) defined as age at which $IOP \geq 22$ mmHg (ocular hypertension: OHT) or at which optic disk degeneration was first detected. Endophenotypes variabilities were tested for their heritability. Genotypes of 408 microsatellites in 184 CA members were analyzed using a Bayesian MCMC method in Loki. A pedigree-based three-stage algorithm was designed to optimize the probability of selecting unequivocal double-mutants, defined as *MYOC*^{K423E} HTZ (affected and asymptomatic) who simultaneously carry potential mutations at the modifier locus.

Results: 156 individuals were found HTZ for *MYOC*^{K423E}, 120 of these were OAG or OHT with treatment. AAO ranged from 7 to 63 years old. The other 36 HTZ were asymptomatic. Only AAO and IOP_{max} showed heritability, both with $h^2 \geq 0.4$. OHT was detected as the 1st symptom and preceded optic nerve damage in $>98\%$ of the affecteds, confirming that AAO was a reliable endophenotype to use for searching modifiers. Our genome-wide linkage analysis mapped a strong modifier locus for AAO at 20q13 with a maximal Bayes Factor = 27. It was named *MOG1* (modifier of glaucoma). Saturation genotyping with SNPs refined *MOG1* to a 9-10 cM interval between D20S857 and D20S430. When comparing the AAOs of the double mutants (*MYOC*^{K423E} HTZ + *MOG1* mutant) with the median AAOs of their respective neighbors (≤ 1 st cousins) who were *MYOC*^{K423E} HTZ but *MOG1* wild-type, the modifier delayed the ages at onset of the double mutants by an average of 10 years.

Conclusions: The *MOG1* locus encodes at least 1 DNA element linked to extreme ages at onset. It delays AAO of glaucoma by an average of 10 years. *MOG1* interacts with *MYOC*^{K423E} mutation most probably by hampering the first manifestations of OHT.

Commercial Relationships: Vincent Raymond, None; Pascal Belleau, None; Rose Arseneault, None; Stéphane Dubois, None; Jean-Louis Anctil, None; Gilles Côté, None; Marcel Amyot, None; Fahed Elian, None; Michael A. Walter, None
Support: Canadian Institutes of Health Research, Vision Research Network of Fonds de Recherche Québec Santé, Fondation des Maladies de l'Oeil, The Glaucoma Foundation USA

Program Number: 3426

Presentation Time: 4:45 PM–5:00 PM

Identification of Novel Genes Required for Eye Function via Systematic Screening of Knockout Mouse Lines by the International Mouse Phenotyping Consortium

*Ala Moshiri*¹, *Bret Moore*², *Ann Cooper*², *Brian Leonard*², *Sydney Edwards*², *Lionel Sebbag*², *Denise Imai*⁴, *Stephen M. Griffey*⁴, *David Clary*³, *Lynette R. Bower*³, *Sara M. Thomasy*², *Terrence Meehan*⁶, *Michel J. Roux*⁵, *Patrick Reilly*⁵, *Yann Herault*⁵, *Christopher J. Murphy*^{2,1}. ¹Ophthalmology, U.C. Davis, Sacramento, CA; ²Veterinary Surgical and Radiological Sciences, UC Davis, Davis, CA; ³Mouse Biology Program, UC Davis, Davis, CA; ⁴Comparative Pathology Laboratory, U.C. Davis, Davis, CA; ⁵PHENOMIN-Institut Clinique de la Souris, Institut de Genetique et de Biologie Moleculaire et Cellulaire, Strasbourg, France; ⁶International Mouse Phenotyping Program, European Bioinformatics Institute, Hinxton, United Kingdom.

Purpose: To identify genes required for normal ocular development and function. Determining the genetic basis of eye development and function remains a major challenge in the diagnosis and treatment of both common and rare blinding diseases. This process requires a spectrum of approaches from human clinical genetics to the utilization of model organisms to direct scientists to potential disease loci. In this manuscript we report a large-scale genetic screen in mice using a phenotype-driven discovery strategy to identify genes required for normal eye function.

Methods: Forward systematic ophthalmic screening of single-gene targeted knockout mouse pipelines across several international sites to pinpoint genes required for various components of ocular anatomy and function. We performed complete ocular examination of all knockout mice produced at the Mouse Biology Program at UC Davis. To maximize the ocular phenotypes detected through all collaborative branches of this knockout mouse project, we interrogated the public data base at www.mousephenotype.org to include all animals with eye related phenotypes.

Results: In summary, we have identified 470 unique genes required for eye development and function. Of these, 308 have no known role in the eye in any species, and are therefore novel. Another 104 genes are known to be expressed in ocular tissues, but are not associated with a known ocular phenotype. The remaining 58 genes have established ocular phenotypes in humans, mice, fish, or other vertebrates. Each of these genes affects one or more ocular structures. The genes have been organized based on the structure(s) affected in the eye.

Conclusions: These genes reveal a number of new molecular pathways potentially involved in human ocular development and disease. We illustrate examples of knockout mouse phenotypes discovered in the screen affecting various compartments of the eye.

Commercial Relationships: *Ala Moshiri*, None; *Bret Moore*, None; *Ann Cooper*, None; *Brian Leonard*, None; *Sydney Edwards*, None; *Lionel Sebbag*, None; *Denise Imai*, None; *Stephen M. Griffey*, None; *David Clary*, None; *Lynette R. Bower*, None; *Sara M. Thomasy*, None; *Terrence Meehan*, None; *Michel J. Roux*, None; *Patrick Reilly*, None; *Yann Herault*, None; *Christopher J. Murphy*, None

Support: RPB Career Development Award, International Retina Foundation Career Development Award

Program Number: 3427

Presentation Time: 5:00 PM–5:15 PM

A Mouse Model of Schnyder Corneal Dystrophy with the N100S Point Mutation

*Fei Dong*¹, *Xueting Jin*², *Michelle Boettler*¹, *Sciulli Harrison*¹, *Mones S. Abu-Asab*³, *Shurong Wang*^{1,4}, *Yueh-Chiang Hu*⁶, *Maria M. Campos*³, *Howard S. Kruth*², *Jayne S. Weiss*⁵, *Winston W. Kao*¹. ¹Ophthalmology, University of Cincinnati, Cincinnati, OH; ²Laboratory of Experimental Atherosclerosis, NIH, Bethesda, MD; ³Histopathology Core Facility, NIH/NEI, Bethesda, MD; ⁴Ophthalmology, the Second Hospital of Jilin University, Changchun, China; ⁵Department of Ophthalmology, Pathology and Pharmacology, Louisiana State University, New Orleans, LA; ⁶Division of Developmental Biology, Cincinnati Children's Hospital Medical Center, Cincinnati, OH.

Purpose: Schnyder corneal dystrophy (SCD) is an autosomal dominant disease in humans, which is caused by mutations in the Ubia prenyltransferase domain containing 1 (*UBIAD1*) gene in chromosome 1 p36 and is characterized by progressive corneal opacification resulting from abnormal deposition of cholesterol and phospholipids. To investigate the pathogenesis and develop therapeutic regimens for SCD, we generated a mutant mouse line carrying a N100S mutation in *Ubiad1*, which mimics human N102S mutation.

Methods: The *Ubiad1*^{N100S} mouse line was generated by the CRISPR/Cas9 genome editing technique. Twenty corneas from ten individual mice of the genotypes *Ubiad1*^{N100S/N100S}, *Ubiad1*^{N100/WT} and wild type (WT) lines were subjected to *in vivo* confocal microscopy (Heidelberg Retinal Tomograph-HRTII Rostock Cornea Module) at the age of 6 weeks. Quantitative analysis of deposits based on *in vivo* confocal microscopic images was conducted using Image J software. Filipin staining was performed on cryosections of *Ubiad1*^{N100S/N100S}, *Ubiad1*^{N100S/WT} and WT mice to determine the cholesterol deposition in cornea. *Ubiad1*^{N100S/N100S}, *Ubiad1*^{N100S/WT} and WT mice corneas were examined with *electron microscopy*.

Results: The *Ubiad1*^{N100S} point mutation mouse line has been successfully created using the CRISPR/Cas9 technique. Homozygous *Ubiad1*^{N100S/N100S} and heterozygous *Ubiad1*^{N100S/WT} mice are fertile and do not manifest apparent pathology except for anterior corneal. Filipin staining demonstrated elevated cholesterol in cornea of *Ubiad1*^{N100S/N100S} and *Ubiad1*^{N100S/WT}. Electron microscopy revealed mitochondrial degeneration in the epithelium and keratocytes. These observations implied that the pathogenesis of SCD might be related to cholesterol accumulation and mitochondrial regulation of lipid metabolism.

Conclusions: The *Ubiad1*^{N100S} mouse provides a promising animal model of SCD which may facilitate understanding SCD pathogenesis and development of therapeutic regimens for SCD.

Commercial Relationships: *Fei Dong*, None; *Xueting Jin*, None; *Michelle Boettler*, None; *Sciulli Harrison*, None; *Mones S. Abu-Asab*, None; *Shurong Wang*, None; *Yueh-Chiang Hu*, None; *Maria M. Campos*, None; *Howard S. Kruth*, None; *Jayne S. Weiss*, None; *Winston W. Kao*, None

Support: NIH/NEI grants RO1 EY011845, RO1 021768, unrestricted Departmental grant of Research to Prevent Blindness and Ohio Eye Research Foundation

Program Number: 3428

Presentation Time: 5:15 PM–5:30 PM

Abnormal ocular development and reduced vision in zebrafish after morpholino-mediated knockdown of *ARHGAP33*

Angela Gauthier^{1,2}, John Borchert¹, Anna Larson¹, Janey L. Wiggs¹.

¹Ophthalmology, Massachusetts Eye and Ear Infirmary, Boston, MA;

²Ophthalmology and Visual Science, Yale School of Medicine, New Haven, CT.

Purpose: Early-onset glaucoma has a strong genetic factor, but only 20% of affected patients have mutations in known disease-causing genes. Whole exome sequencing of 27 early-onset glaucoma families found 3 families with *ARHGAP33* mutations, suggesting *ARHGAP33* as a promising candidate. This study explores the functional impact of *ARHGAP33* mutations by using morpholino-mediated knockdown of the *ARHGAP33* ortholog in zebrafish embryos.

Methods: Embryos at the 1-8 cell stage were injected with 2-3 nL of 0.4mM *ARHGAP33* translation-blocking (TB), 0.4 mM *ARHGAP33* splice-site blocking (SS), or 0.5 mM standard (STD) control morpholinos, and one group was uninjected (UI). Eye area, head area, and body length were measured at 3 days post fertilization (dpf).

Vision was studied at 5 dpf by visual motor response (VMR), a device that measures activity levels in response to light change.

Results: Each group included approximately 100 embryos, and survival at 5 dpf was 37% for TB, 45% for SS, 53% for STD, and 84% for UI. STD and UI had no differences in eye area ($66,481 \pm 4,245 \text{ mm}^2$ and $66,942 \pm 4,067 \text{ mm}^2$, $p = 0.65$), eye/head area (0.25 ± 0.02 and 0.25 ± 0.01 , $p = 0.49$), and body length ($3,408 \pm 116 \text{ mm}$

and $3,458 \pm 100 \text{ mm}$, $p = 0.08$). STD and SS also had no differences in these variables ($66,041 \pm 4,245 \text{ mm}^2$, $p = 0.76$; 0.25 ± 0.02 , $p = 0.87$; $3,355 \pm 120 \text{ mm}$, $p = 0.15$). 50% of TB fish had a severe phenotype of significantly smaller eye area ($31,903 \pm 7,686 \text{ mm}^2$, $p < 0.001$), eye/head area (0.19 ± 0.04 , $p < 0.001$), and body length ($1,858 \pm 295 \text{ mm}$, $p < 0.001$) than STD. The remaining TB fish also had a significantly smaller eye area ($57,568 \pm 2,415 \text{ mm}^2$, $p < 0.001$) and body length ($2,768 \pm 424 \text{ mm}$, $p = 0.04$) than STD but had no difference in eye/head area (0.26 ± 0.02 , $p = 0.19$).

VMR testing of 24 fish from each group showed no difference between the SS, STD, and UI fish. Severe phenotype TB fish had no baseline movement due to skeletal dysmorphology. When these were excluded, the TB fish still did not show a significant activity spike in response to light, unlike the other groups.

Conclusions: The *ARHGAP33* TB morpholino had a significant negative effect on zebrafish eye and body development and vision. *ARHGAP33* knockout mice have been shown to express less TRKB, which is needed for retinal ganglion cell survival. Together, these findings suggest a possible role for *ARHGAP33* in glaucoma-related neurodegeneration.

Commercial Relationships: Angela Gauthier, None;

John Borchert, None; Anna Larson, None; Janey L. Wiggs, None

Support: Yale School of Medicine One Year Medical Student Research Fellowship, March of Dimes Foundation, NIH/NEI P30 EY014104